

# VACUUM CHARACTERIZATION AND IMPROVEMENT FOR THE JEFFERSON LAB POLARIZED ELECTRON SOURCE\*

M.L.Stutzman<sup>#</sup>, P.A.Adderley, M.Poelker, Jefferson Lab, Newport News, VA 23606, USA  
 Md.A.Mamun, Old Dominion University, Norfolk, VA 23529 USA

## Abstract

Operating the JLab polarized electron source with high reliability and long lifetime requires vacuum near the XHV level, defined as pressure below  $7.5 \times 10^{-13}$  Torr. This paper describes ongoing vacuum research at Jefferson Lab including characterization of outgassing rates for surface coatings and heat treatments, ultimate pressure measurements, investigation of pumping including an XHV cryopump, and characterization of ionization gauges designed for this pressure regime.

## MOTIVATION

The Jefferson Lab polarized electron source delivers an electron beam with polarization near 90% from a 130 kV DC high voltage electron gun. Lifetime is limited by the residual gasses in the system. These gasses are ionized by the electron beam and accelerated into the strained-superlattice photocathode, causing both ion implantation and affecting surface chemistry [1]. To enhance photocathode lifetime, and with the goal of developing higher current guns for future applications, a series of vacuum research measurements is underway. The pressure in a system is determined by the amount of gas entering the system and the effective removal of gas with pumps. As such, lower pressure can be obtained by reducing the gas load, which is dominated by hydrogen outgassing in UHV systems like photoguns, and/or increasing the pump speed. We describe our efforts to reduce outgassing and enhance pumping below. Furthermore, we discuss the challenges associated accurate pressure monitoring near the XHV regime.

## OUTGASSING RATE STUDIES

Once a stainless steel vacuum chamber is baked to remove water vapor, the dominant gas in the chamber is hydrogen that originates from outgassing from the chamber walls. Measurements of the outgassing rate of small steel test chambers were made to determine the efficacy of reducing outgassing via medium temperature bakeouts, and by applying coatings to the chamber walls [2]. Two coatings were studied: titanium nitride (TiN) and amorphous silica (a-Si). Outgassing rates were measured for each system using a spinning rotor gauge and a gas accumulation method [3]. The lowest outgassing rates (at the room temperature of 25°C) are shown in Figure 1. Each value represents a significant outgassing rate reduction compared to the  $1 \times 10^{-12}$  TorrLs<sup>-1</sup>cm<sup>-2</sup> outgassing

rate typical of stainless steel that has undergone conventional 250°C bakeout.

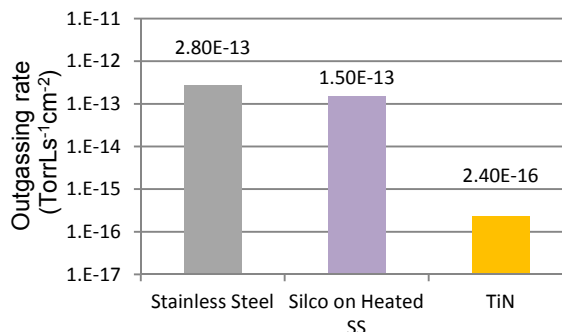


Figure 1: Best outgassing rate achieved for each chamber at room temperature of 25°C: the bare steel (304L stainless steel), the a-Si coating on 400°C heat treated steel, and the TiN coating.

## BASE PRESSURE MEASUREMENTS

These outgassing rate values were inserted into the simple equation,  $P = \frac{qA}{S}$ , to predict the expected ultimate pressure P (Torr) that could be achieved for a given pump speed S (L/s), where q is the outgassing rate in TorrLs<sup>-1</sup>cm<sup>-2</sup>, and A is the internal area of the chamber in cm<sup>2</sup>. Pumping for each chamber was provided by an ion pump [4] and non-evaporable getter modules [5], for a total pump speed of 1680 L/s. Following installation of pumps and bakeout, the pressure was measured using gauges with commercially rated for the XHV pressure range.

Table 1

Chamber	Expected Pressure (Torr)	Measured Pressure (Torr)
Stainless Steel	$8.6 \times 10^{-13} \pm 3 \times 10^{-13}$	$9.4 \times 10^{-13} \pm 4 \times 10^{-13}$
TiN Coating	$7.3 \times 10^{-16} \pm 3 \times 10^{-13}$	$1.0 \times 10^{-12} \pm 5 \times 10^{-13}$
a-Si coating	$4.6 \times 10^{-13} \pm 2 \times 10^{-13}$	$1.7 \times 10^{-12} \pm 8 \times 10^{-13}$

From Table 1, measured and predicted pressures are in reasonable agreement for the bare stainless steel and a-Si chambers. However, the measured pressure for the TiN system is greater than predicted pressure by three orders of magnitude. This can be understood by a careful examination of both the TiN coating chemical

\*Work supported by U.S. DOE Contract No. DE-AC05-06OR23177 and with funding from the DOE R&D for Next Generation Nuclear Physics Accelerator Facilities Funding Opportunity Number: DE-FOA-0000339.

#marcy@jlab.org

composition and an understanding of the SRG outgassing rate measurement.

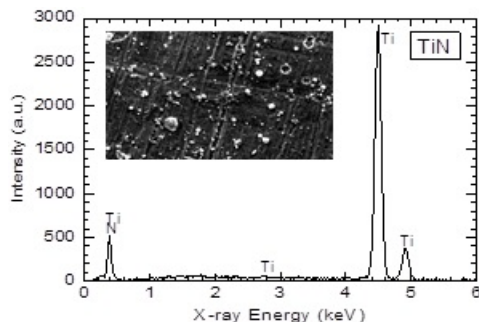


Figure 2: XPS analysis of the Ti:N coating, showing prevalence of Ti and N in the coating, and SEM image inset showing inhomogeneity in the coating.

An XPS analysis of the TiN coating shows the presence of both Ti and N as expected, and the average stoichiometric ratio is 1:1 Ti:N, but there exists significant inhomogeneity in the coating, with Ti:N ratios anywhere from 0.58:1 up to 1.17:1. Since elemental Ti is a well-known pump for hydrogen, the existence of elemental hydrogen in the coating would potentially provide some pump speed in the system. The accumulation method of outgassing rate measurement requires that there is no pump speed in the system under test, and that all the gas evolving from the surface causes the pressure rise in the chamber. A pump speed from the TiN coating of as little as 0.003 L/s would result in an erroneous low outgassing rate, and reconcile the discrepancy between the measured base pressure and the base pressure predicted by the extraordinarily low outgassing rate.

### XHV GAUGES

The measurement of pressures below  $1 \times 10^{-11}$  Torr requires specially designed gauges. The background contributions in a typical Bayard-Alpert gauge include an x-ray limit [6], electron stimulated desorption [7] and gauge heating effects [8]. Several gauges have been designed to minimize these effects, such as the extractor gauge [9,10], the AxTran gauge [11], and the Watanabe Bent Belt Beam gauge (3BG) [12]. These three gauges were used in combination to characterize the gauge performance, measure the background contributions to each gauge signal, and provide confidence in the measured pressure at values at or below  $1 \times 10^{-12}$  Torr. The x-ray limit was measured for each gauge, [6] by varying the ion steering voltages such that no electrons or ions could reach the collector. The residual current is the x-ray limit. For the extractor gauge, the x-ray generated contribution represents a significant portion of the total collector current at pressures described here (see Figure 3), making the measurement and subtraction of this background essential. The 3BG had no measurable x-ray background, as expected from the design with no line of sight between grid and collector. The Bessel box design of the AxTran gauge also yields an x-ray induced background consistent with zero.

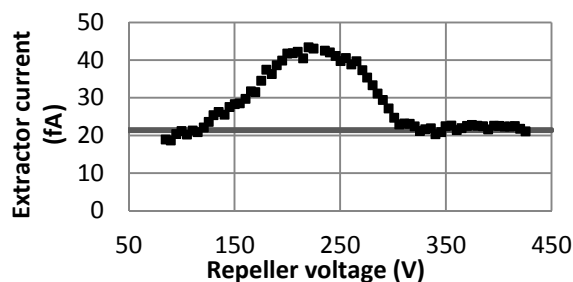


Figure 3: Measurement of the x-ray limit for an extractor gauge. The x-ray limit was measured by varying the repeller voltage on an external power supply and measuring the collector current. For increased sensitivity, the collector current was measured on an electrometer. The pressure during this measurement was in the low  $10^{-12}$  Torr range, with an x-ray limit of approximately  $1 \times 10^{-12}$  Torr.

The contribution due to gauge heating effects was evaluated by alternately turning gauges on and off while monitoring pressure with a neighboring gauge. Figure 4 shows a typical example, indicating a pressure reduction of  $\sim 1 \times 10^{-12}$  Torr when the extractor gauge was turned off. Similar results were obtained for each gauge.

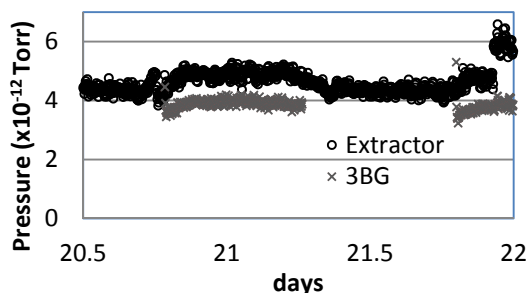


Figure 4: Study of gauge heating effect by measuring pressure in a chamber while one gauge was turned on and off. Note the time scale of days to let the system settle between state changes.

For all gauges, the magnitude of the gauge heating effect was on the order of  $1 \times 10^{-12}$  Torr, making this a significant effect for each gauge at XHV pressures. The final contribution to gauge current that is not related to the pressure is due to the desorption of gas from the gauge [7]. Gauges such as the AxTran are designed to be able to discriminate between ESD ions and gas phase ions [11], but in practice degassing the gauges and waiting a significant amount of time, on the order of weeks, allowed the pressure to stabilize and the ESD effects to be minimized in each system.

### XHV PUMPING

The JLab polarized electron gun has successfully used a combination of ion and NEG pumps for more than a decade to achieve pressures in the low  $10^{-12}$  Torr range (as measured by an extractor gauge, taking the x-ray limit into account). With the introduction of the Leybold XHV

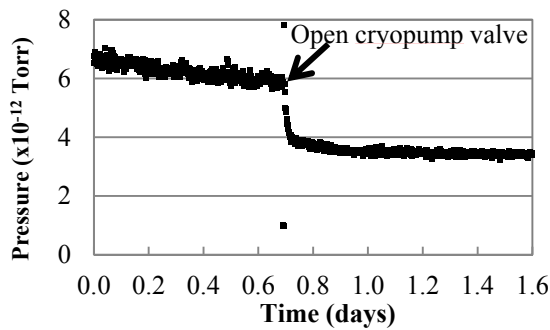


Figure 5: The pressure of the cryopump test stand as the valve was opened to the cryopump. Prior to opening the valve, the system was pumped with a combination of NEG and ion pumps. The pressure was measured using an extractor gauge, with an x-ray limit of approximately  $1 \times 10^{-12}$ , and gauge heating of similar magnitude, which have not been subtracted yet from the data shown in the plot.

bakable cryopump, we designed a series of experiments to determine if the cryopump alone or in combination with the NEG and ion pumps could yield a significant improvement in base pressure of a system.

Cryopumps require a large surface area such that the adsorbed gasses are able to stay at coverages below a monolayer. Without this large surface area, even at temperatures at 4 or 10K, the partial pressure of common gasses once they reach more than monolayer coverage [13] becomes much higher than is acceptable for a UHV/XHV system (for example, hydrogen partial pressure at 4.2K is over  $1 \times 10^{-7}$  Torr with more than a monolayer adsorbed). Traditionally, charcoal from coconuts has been found to be an excellent cryosorbent material, but the low temperature compatible adhesives used to hold charcoal to the cold surfaces of a cryopump are typically incompatible with bakeouts to remove all water vapor from a cryopump. Thus, cryopumping has typically been limited to pressures above  $1 \times 10^{-10}$  Torr.

The Leybold bakable XHV cryopump overcomes this inability to bake a cryopump by using a  $\text{LN}_2$  chill circuit that enables the adhesive and compressor mechanical systems to be kept below their high temperature limits (typically  $50^\circ\text{C}$ ) during a bakeout of the cryopump housing.

Using a chamber the size of the JLab electron gun, heat treated at  $400^\circ\text{C}$ , we measured the pressure in the system when the cryopump was added to the typical NEG/ion pump combination.

Figure 5 shows the effect of opening the NEG/ion pumped chamber to the cryopump. Although lower pressure was achieved using the cryopump, measured pressure both with and without the cryopump was considerably higher than expected (Table 2), even taking into consideration the large, non-heat-treated surface area of the gate valve and conductance limitation calculations between the chamber and the pump. In situ gauge characterization and careful consideration of outgassing

from thick flanges and internal hardware will be taken into account to reconcile calculations and measurements.

Additionally, further work is required to determine if the magnitude of the improvement justifies the additional complexity for future electron sources, and if there are limitations in the ion pump or the NEG pumps that can be solved using the cryopump either alone or in combination. Finally, in practice, this closed cycle helium compressor system has significant vibration, and this as well as other engineering issues would need to be resolved if the improvement in the pressure gained by adding an XHV cryopump is deemed worthwhile.

Table 2

	NEG, ion	NEG, ion, cryo
Getter pump (l/s)	2150	2150
Ion pump (l/s)	45	45
Cryopump (l/s)	-	800-1300 (conductance dependent)
Area ( $\text{cm}^2$ )	8000 (chamber)	8000 (chamber) 3400 (bellows) 13700 (gate valve)
Outgassing ( $\text{TorrLs}^{-1}\text{cm}^{-2}$ )	$1 \times 10^{-13}$	$\geq 1 \times 10^{-13}$
Expected Pressure	$4 \times 10^{-13}$ Torr	$3 - 7 \times 10^{-13}$ Torr
Achieved pressure	$4 \times 10^{-12}$ Torr	$1.5 \times 10^{-12}$ Torr

## CONCLUSIONS

Ongoing vacuum research points toward several conclusions regarding improving vacuum into the XHV regime with the goal of improving photocathode lifetime by reducing ionization of residual gasses and bombardment of the photocathode by these ions. First, heat treatment alone of a steel chamber is as effective as either of the surface treatments that were tested: the very low measured TiN outgassing rate was likely an artifact of a small pump speed in the coating, made evident by the discrepancy between measured and achieved base pressure in the systems. Gauge backgrounds must be characterized before pressure measurements near the XHV regime can be considered reliable. Finally, the XHV cryopump does improve the vacuum of a system pumped with NEG and ion pumps, but with a significant amount of added complexity and expense to the system, and work continues to understand the benefits and limitations of the cryopump as an XHV pump for electron source applications.

## REFERENCES

- [1] V. Shutthanandan, Z. Zhu, M.L. Stutzman, F.E. Hannon, C. Hernandez-Garcia, M.I. Nandasiri, S.V.N.T. Kuchibhatla, S. Thevuthasan, W.P. Hess., Phys.Rev.ST Accel.Beams **15** 063501 (2012).
- [2] Md. A. Mamun, A. A. Elmustafa, M. L. Stutzman, P. A. Adderley and M. Poelker, J. Vac. Sci. Technol. A **32**, 021604 (2014).

- [3] P.A. Redhead, *J.Vac.Sci.Technol.A* **20** 1667 (2002).
- [4] Gammavacuum.com, 45 L/s TiTan DI, SEM/XHV style pump used.
- [5] saesgetters.com, SAES WP1250, ST707 material
- [6] F. Watanabe *J.Vac.Sci.Technol.A* 9 2744 (1991).
- [7] P.A.Redhead, *Vacuum* 48 585 (1997).
- [8] F. Watanabe *J.Vac.Sci.Technol.A* 20 1222 (2002).
- [9] P.A.Redhead, *J.Vac.Sci.Technol.* 3 173 (1966).
- [10] Commercial extractor gauge distributed by oerlikon Leybold vacuum, Ionivac IM 540 with the IE 514 sensor. <http://www.leyboldproducts.oerlikon.com/>
- [11] N. Takahashi et al., *J.Vac.Sci.Technol.A* 23 554 (2005). Commercial gauge distributed by UlVac, <http://www.ulvac.com>
- [12] F. Watanabe *J.Vac.Sci.Technol.A* 28 486 (2010).
- [13] K. Jousten, ed., "Handbook of Vacuum Technology", (Berlin:Wiley, 2008), p. 530.